

# Millimeter Wave Reconfigurable Metasurface Intelligent Reflecting Surface Based on Piezoelectric Crystal for 5<sup>th</sup> and 6<sup>th</sup> Generation of Wireless Communication

Asaf Barom\*, Efi Rahamim, Daniel Rozban, David Rotshild, Amir Abramovich

Department of Electrical and Electronic Engineering, Ariel University, Ariel, Israel

Email: \*asaf8040@gmail.com

**How to cite this paper:** Barom, A., Rahamim, E., Rozban, D., Rotshild, D. and Abramovich, A. (2022) Millimeter Wave Reconfigurable Metasurface Intelligent Reflecting Surface Based on Piezoelectric Crystal for 5<sup>th</sup> and 6<sup>th</sup> Generation of Wireless Communication. *Communications and Network*, 14, 109-118.

<https://doi.org/10.4236/cn.2022.144008>

**Received:** June 28, 2022

**Accepted:** November 2, 2022

**Published:** November 15, 2022

Copyright © 2022 by author(s) and Scientific Research Publishing Inc. This work is licensed under the Creative Commons Attribution International License (CC BY 4.0).

<http://creativecommons.org/licenses/by/4.0/>



Open Access

## Abstract

The new requirements from the 5<sup>th</sup> and the 6<sup>th</sup> generation of wireless communication are ultra-high data rate, energy efficiency, wide coverage and connectivity, high reliability, and low latency. The current technologies cannot achieve all the mentioned requirements. New technologies and new approaches for deploying more active and passive nodes must be developed. Furthermore, the use of MMW band and THz band (30 - 300 GHz), in order to utilize their huge bandwidth, results in deploying more active node and more antennas due to high propagation losses and “LOS” behavior at this band. Development of innovative technologies is necessary to realize the above demand for growth of future wireless communication. The main task is to suggest solutions for the time varying characteristic of the wireless channel due to the user mobility and shadowing or blocking of communication channel. The current methods such as use of pilot channel to estimate the fading, various modulation or coding and beamforming, have overhead and limitations over random (large, unexpected changes) channels.

## Keywords

Wireless Communication, Metasurface, Intelligent Reflection Surface (IRS), Millimeter Wave (MMW)

## 1. Introduction

In this study we propose Intelligent Reflection Surface (IRS) as part of modern wireless networks. The IRS can enhance the performance of future wireless com-

munication deployment. The main advantageous of the IRS are very low-cost, no need for RF chains, enables Full Duplex (FD) operation, very light weight and very flexible. Thus, the IRS is suitable for deployment in future wireless communications. **Figure 1** shows the deployment of Massive MIMO (M-MIMO) wireless network in open space. The discrimination and beamforming between the users are done by the M-MIMO base station. In this case the M-MIMO Base Station BS is very expensive and complicated.

In Urban region it cannot be implemented this way due to obstacles and barriers in the Line Of Sight (LOS) between the M-MIMO base station and the user especially for MMW and THz radiation which will be used in the future for their huge bandwidth. However, it can be implemented using IRS. Furthermore, a much simpler base station is required in this case as shown in **Figure 2** for the same users locations as shown in **Figure 1**. For example, user A (**Figure 1** and **Figure 2**) and user B (**Figure 1** and **Figure 2**) are in the same position relative to the base station. In urban (**Figure 2**) There is no LOS between those users and

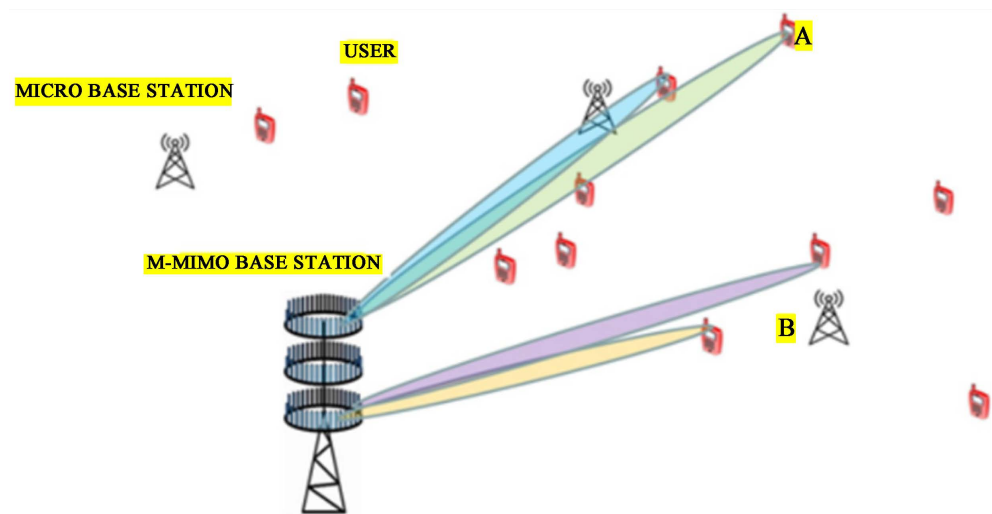


**Figure 1.** Open space M-MIMO wireless communication network.

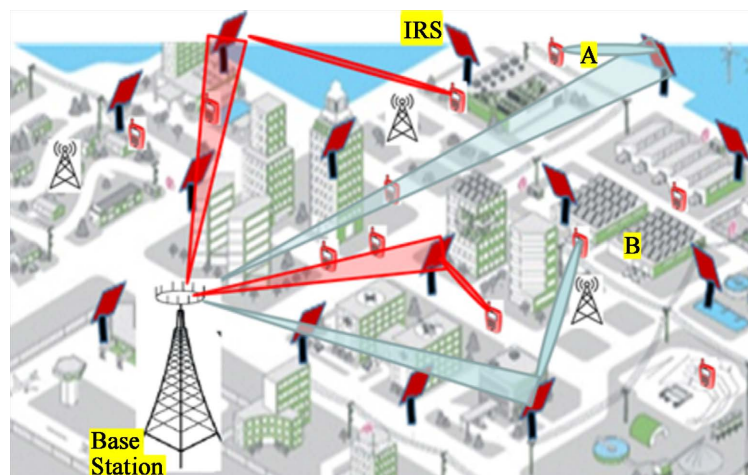


**Figure 2.** Urban region base station and IRS wireless communication.

the BS, compared to open space shown in **Figure 1**. The IRS enables virtual LOS and high-quality beamforming as demonstrated in **Figure 2**.

An innovative W band (75 GHz - 110 GHz) MetaSurface (MS) IRS for future wireless communication is suggested in this study. Meta-Materials (MM) are materials having a unique electromagnetic properties not existing in nature. The difference between the MM and the new materials made up of synthetic molecules is in the engineering-geometric structure. While many other synthetic molecules are unique in their chemical structure the MM novelty is the spatial arrangement of individual “molecules,” which are known as unit cells or meta-atoms. Meta Surface (MS) is a 2D version of MM that has electromagnetic properties not existed in nature. In recent years, a large amount of research has been conducted in the field of MS, enabling fascinating electromagnetic properties that cannot be achieved with naturally occurring materials. In contrast to conventional materials, metasurfaces allow for a new way to manipulate microwave and MMW radiation based on reflection from sub-wavelength unit cells periodic array, having simultaneously negative permeability and permittivity [1] [2] [3]. Adding tunability element to each unit cell of the MS enables steering the reflected beam direction of an incident beam in a specific frequency band. Examples for such reconfigurable MS reflector for sub 6 GHz band are shown in [4] [5] for X-band studies [6] [7] and for Ka-band shown in [8]. Previous studies have used tuning elements such as Varactor Diodes which were very popular as a tuning element for the low MMW range. However, the move to the high MMW (W-BAND) domains places high demands on the tuning element and the use of Varactor Diodes as the tuning element is no longer relevant because they cannot work in the range exceeding 40 GHz. The new design presented in this study enables manufacturing of a MS IRS with a reconfigurable steering ability in W-band for wireless communication applications [9]. This IRS will be based on metasurface principle and piezoelectric (PE) crystal as the tunable element. The possibility of using a piezoelectric crystal for the purpose of adjusting the return beam for high frequency is shown in [10]. Moreover, mention that the active elements add an extra, and dynamically variable, degree of freedom in any of the metasurface parameters to produce a tunable reflected response. Various tunable components have been previously proposed and more recently piezoelectric actuators.

## 2. Unit Cell Design

The unit cells structure scheme, which interacts with the field components of the incidence plane wave, and the basic equivalent circuit model of the unit cells structure, are given in **Figure 3**.

**Figure 3(a)** shows the basic unit cells structure, which is consisted of a dielectric substrate with a geometric metal shape such as patches, slots, rings, or more complex geometries printed on its top, such as K-shape [12], connected by via to a metal surface at the bottom of the dielectric substrate used as ground plane

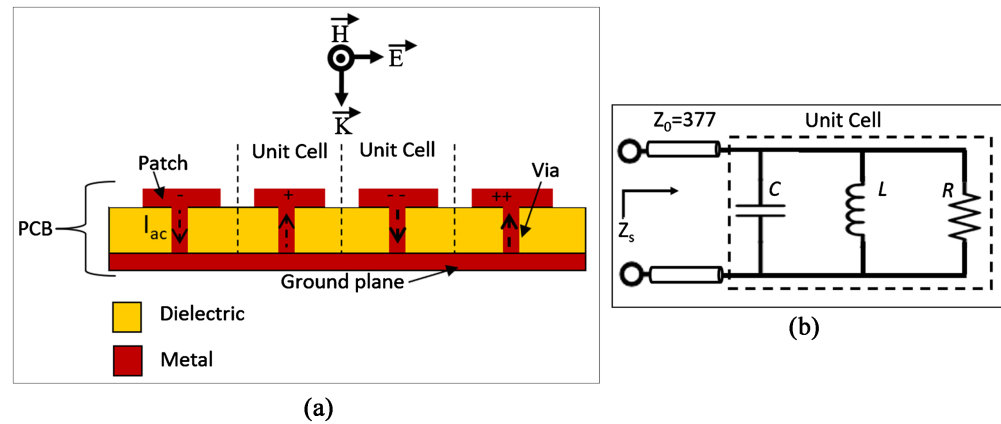


**Figure 3.** Basic unit cell model (a) side description of the unit cell layer structure in interaction with plane wave (b) unit cell equivalent circuit model [11].

(see **Figure 3(a)**). **Figure 3(b)** presents a unit cell analysis as an equivalent parallel resonant circuit of lumped elements [12].  $Z_0$  is the typical impedance in a vacuum, and it constitutes the resistance which the wave sees in its entry into the circle. An example of designing a patch shape geometry meta cell is presented in [13]. In this study [13] an MMW flat parabolic mirror was design, constructed and tested. This FLAPS design is based on an array of variable-dimension metal cells (a metasurface), which are connected to the ground plane through a dielectric substrate. The dielectric constants of the substrate and size of each metal cell determine its electrical characteristics, such as capacitance and inductance, as well as its electromagnetic properties [14]. MMW radiation incident to the FLAPS mirror surface causes currents to flow from the top surface of the dipoles to the ground plane through a passive array of capacitors and inductors, which cause a phase shift in the reflected electromagnetic wave (**Figure 4**). By varying the size of a dipole, we basically vary its phase shift, depending on its location on the FLAPS mirror surface (see **Figure 4**). In this study, the metasurface mirror structure was composed of an FR4 dielectric substrate with a ground plane in the back and printed metal patterns on the front. Each metal cell on the front is connected to the back ground plane by a via, which is coated by a micron layer of copper to enable electrical conductivity from the metal cell to the ground plane (see **Figure 4**). Unlike a unified ground plane, the dimensions of the metal cells on the front are variable. The metal cells in the center are the largest, and they gradually decrease in size as they approach the edges of the FLAPS mirror. The FLAPS mirror cells can be described as an array of parallel LC resonance circuits (illustrated in **Figure 4**) [13]. The capacitance  $C$  is created due to the dielectric gap between two adjacent metal pads, and the inductance  $L$  is created due to the current path through the metal pads and the via.

Piezoelectric materials enable continuously change the unit cell thickness depending on the DC voltage [10]. Thus, the properties of the MS continuously change as well. Using the piezoelectric method is limited because it involves a physical change in the unit cell size and in the structure as can be seen in **Figure 5**.

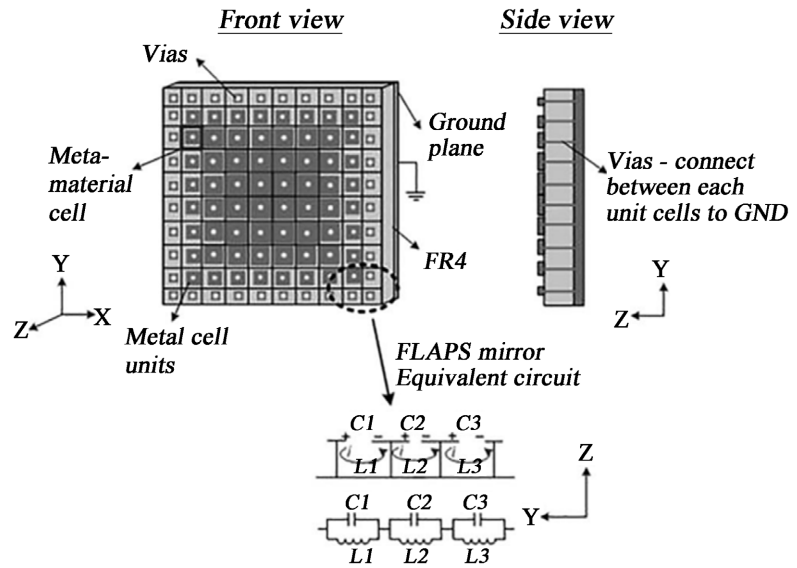


**Figure 4.** Proposed reflector structure composed of an FR4 dielectric substrate with a ground plane and printed metal patterns on the front. Each metal cell on the front is connected to the back ground plane by a via. The metal cells in the center are the largest, and they gradually decrease in size as they approach the edges of the FLAPS mirror.

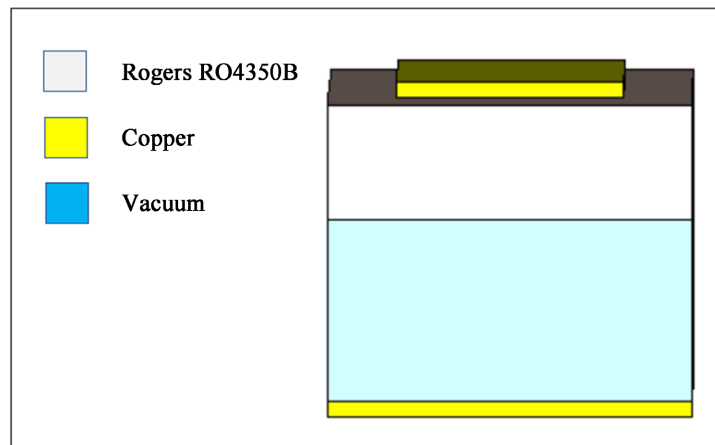


**Figure 5.** Basic unit cell model—side description of the unit cell.

In addition, a high voltage of up to 200 V is needed for control [10]. As can be seen in **Figure 5** the unit cell structure measuring  $0.8 \text{ mm} \times 0.8 \text{ mm}$ . The cell consists at the bottom of a layer of copper with a thickness  $t$ , above it a vacuum layer of thickness  $G$  that allows the movement of the adjusting element and a dielectric substrate Rogers RO4350B with a thickness  $s$ . The dimensions of the layers mentioned are  $W \times W$ . Finally, on top is another layer of copper in thickness  $t$  with  $W_p \times W_p$  dimensions smaller than that of the cell. **Table 1** shows the sizes of the parameters that make up the unit cell.

The “IRS” is supposed to have a free ground surface to allow the dynamic change between the ground and the reflected surface, so the use of “via” is not possible as the two surfaces will be connected and will not be able to make a change. In **Figure 5**, the soil substrate is made of copper, as is the patch the air

is marked in light blue and is made of vacuum, while the dielectric substrate is marked in white. To illustrate the future use of the directional element, simulations were performed for several vacuum thicknesses ( $G = 1.6$  mm,  $G = 1.8$  mm,  $G = 2$  mm,  $G = 2.2$  mm). The change in parameter  $G$  changes the distance from the upper copper to the ground surface, the change in distance affects the capacitance and inductance and determines the resonant frequency [11]. **Figure 6** and **Figure 7** shows how the resonant frequency and phase change depending on the vacuum thickness.

**Figure 6** and **Figure 7** shows that the use with the piezoelectric crystal as a tunable element can be used for deal with high frequencies beamforming, while causing small losses and very wide angular coverage.

### 3. IRS Design

When the unit cells are arranged in a 2-D periodic configuration, the MS are characterized by an effective surface impedance, which was characterized by Dan Sievenpiper work [4] with the surface impedance parameter  $Z_s$ , which is described in Equation (1).

**Table 1.** Parameters of the unit cell.

Parameters	Description	Value (mm)
$W$	Unit cell size	0.8
$W_p$	Patch size	0.5
$t$	Copper thickness	0.035
$G$	Vacuum thickness	1.8
$s$	dielectric substrate thickness	0.254

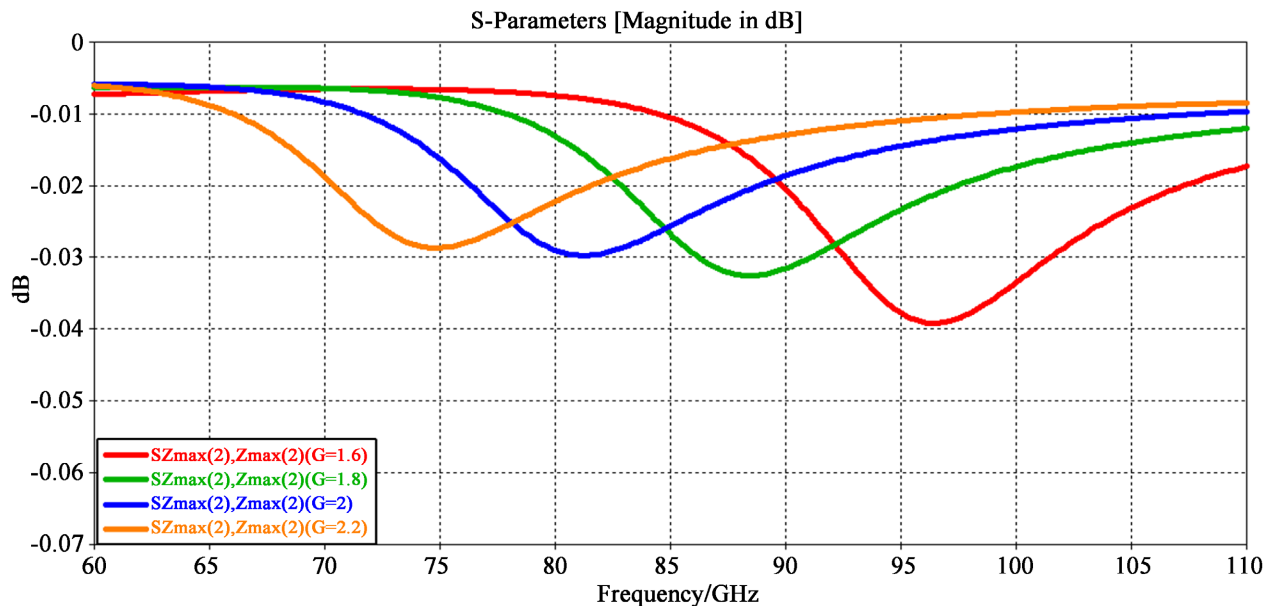


**Figure 6.** S-Parameters (Magnitude) simulation results for IRS unit cell.

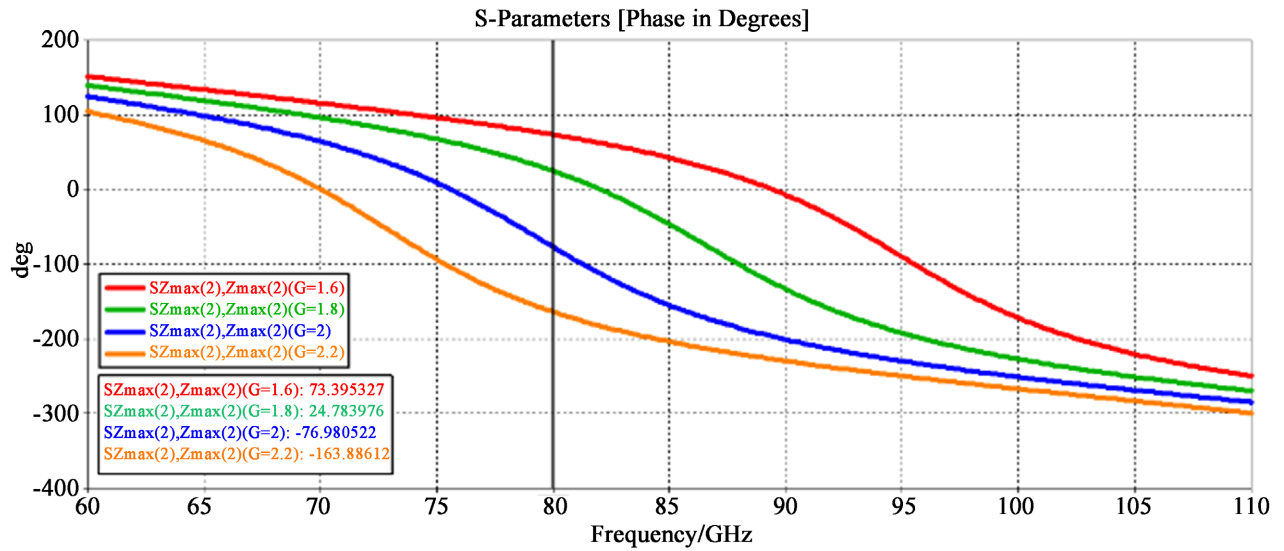


**Figure 7.** S-Parameters (Phase) simulation results for IRS unit cell.

$$z_s = \frac{1}{\frac{1}{R} + j\left(\omega C - \frac{1}{\omega L}\right)} \quad (1)$$

where around the angular frequency values of  $\omega = 1/\sqrt{LC}$  the imaginary part of the  $Z_s$  becomes dominant and is shown in Equation (2).

$$z_s = \frac{j\omega L}{1 - \omega^2 LC} \quad (2)$$

The unit cell values of  $C$  and  $L$  are determined by the unit cell dimensions, geometry, materials, and PCB properties. The parallel resonance frequency of the circuit model around which the radiation is manipulated is shown in Equation (3).

$$f_{res} = \frac{1}{2\pi\sqrt{LC}} \quad (3)$$

The bandwidth of the resonance frequency [15] is shown in Equation (4) and the Q-factor is shown in Equation (5) when the total unit cell losses are given by  $R \times Q$  [4].

$$Bw = \frac{1}{Rc \cdot \omega_0} = \frac{L\omega_0}{R} \propto \frac{L}{C} \quad (4)$$

$$Q = \frac{1}{Bw} \quad (5)$$

The IRS cells can be described as an array of parallel LC resonance circuits (illustrated in **Figure 3(b)**) [13]. The capacitance  $C$  is created due to the dielectric gap between two adjacent metal patches, and the inductance  $L$  is created due to the current path through the metal patches and the via. The value of the capacitance is determined by the dimensions of the copper patch,  $l$ , the substrate thickness ( $h$ ), the gap between adjacent patches ( $W$ ), the vacuum permittivity ( $\epsilon_0 = 8.8541878$  pF/m), and the permittivity of substrate ( $\epsilon_r$ , at W-band). The induc-

tance value,  $L$ , however, is determined by the permeability constant ( $\mu_0 = 1.2566 \mu\text{h/m}$ ,  $\mu_r = 1$ ), and the substrate thickness. The relations for the capacitance and inductance for metal Patch shape unit cell are given by Equations (6) and (7).

$$L = \mu_0 \mu_r h \tag{6}$$

$$C = \frac{l \epsilon_0 (1 + \epsilon_r)}{\pi} \cosh^{-1} \left( \frac{2l + w}{w} \right) \tag{7}$$

The proposed IRS in this study is compose of 2-D Patch shape unit cell, a rotated ground plan and two bend piezoelectric elements. **Figure 8** shows a scheme of the proposed metasurface ISR. As can be seen in **Figure 8**, the ground plain can be rotated according to the PE benders position creating a different distance between the patch according to its position.

The reflected phase and magnitude of each unit cell for different thickness ( $t$ ) can be seen in **Figure 9** [10]. This difference in  $t$  cause to reflected phase gradient

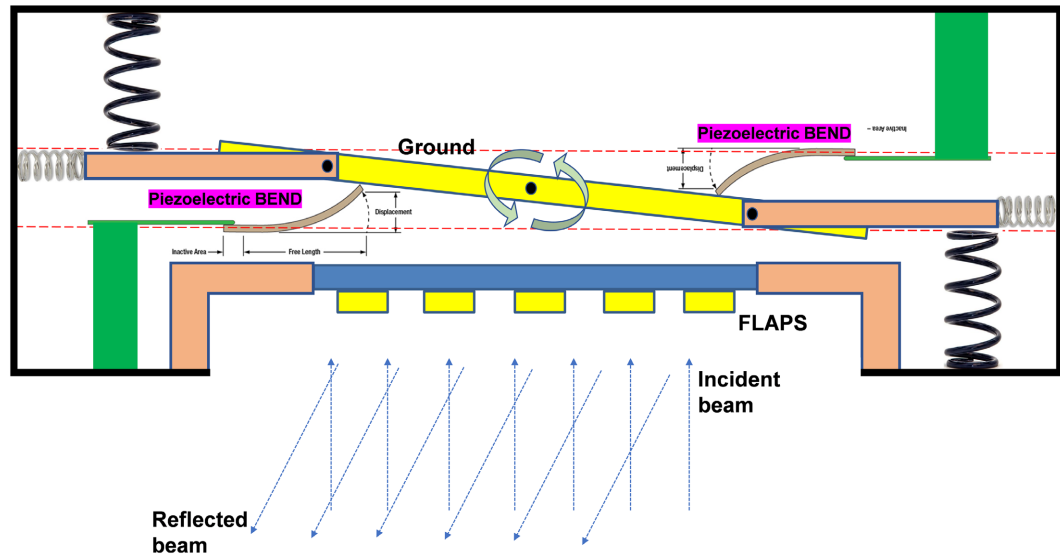


**Figure 8.** A scheme of the proposed metasurface IRS based of PE bender element.

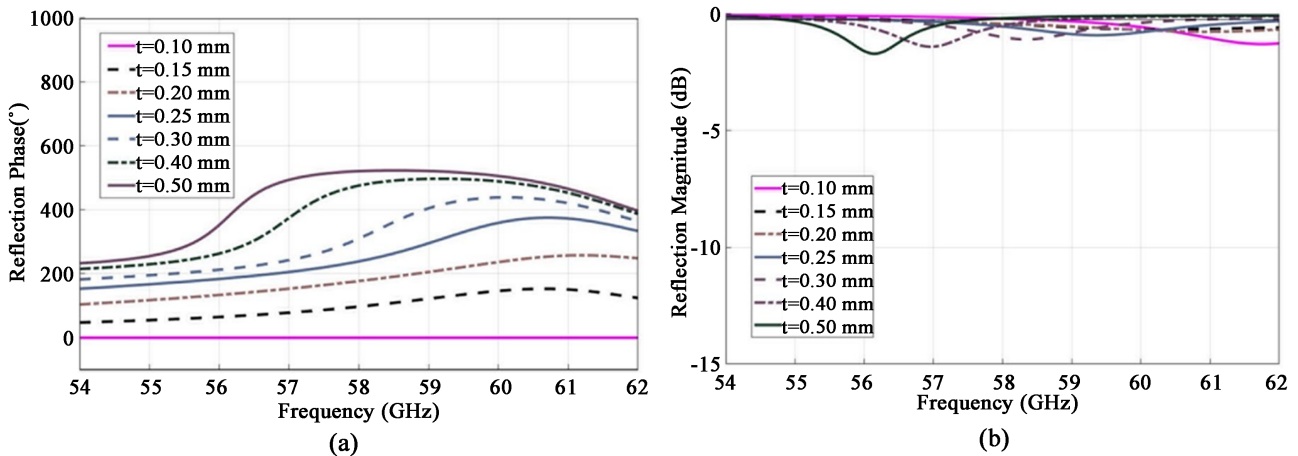


**Figure 9.** Different  $t$  (thickness) values, (a) the phase of the reflection coefficient of the spatial phase as a function of frequency and. (b) The reflection magnitude [dB] as a function of frequency [10].

and to reflected beam angle of  $\theta$  relative to the normal incident beam which range  $\theta > 360^\circ$  phase shift is achieved (see **Figure 9(a)**). Very low losses demonstrate an average loss of 0.5 dB across the operating bandwidth between 57 and 62 GHz are shown in **Figure 9(b)**.

The IRS proposed in this study requires only two voltage sources, one for each piezoelectric crystal. A small number of sources means a significant reduction in the production costs of the IRS surface. Also, the response time of the IRS is faster because of the use of two sources that create the change in inductance and capacitance for all the cells on the surface.

#### 4. Future Plans

For the design of the proposed metasurface IRS we examine different geometric shapes for the final decision that the use of the Patch form is the ideal shape. Then we will work on designing an array that includes about 10,000 cells ( $100 \times 100$  mm). In the final part, we will move on to the IRS production and connect it on top of the mechanical device that will include the use of the piezoelectric crystal for the purpose of deflecting the radiation.

#### Acknowledgements

I would like to thank Professor Amir Abramovitch who took me with him and exposed me to the future and groundbreaking technology. In addition, thanks to Ceragon Network and the Ministry of Economy (Israel) who fund our research and allow us to move forward.

And of course thanks to COMCAS 2021 Conference which gives me the stage to present in an international forum the research work I am working on.

#### Conflicts of Interest

The authors declare no conflicts of interest regarding the publication of this paper.

#### References

- [1] Veselago, V. and Narimanov, E. (2006) The Left Hand of Brightness: Past, Present and Future of Negative Index Materials. *Nature Materials*, **5**, 759-762.  
<https://doi.org/10.1038/nmat1746>
- [2] Holloway, C.L., Kuester, E.F., Gordon, J.A., *et al.* (2012) An Overview of the Theory and Applications of Metasurfaces: The Two-Dimensional Equivalents of Metamaterials. *IEEE Antennas and Propagation Magazine*, **54**, 10-35.  
<https://doi.org/10.1109/MAP.2012.6230714>
- [3] Shelby, R.A., Smith, D.R. and Schultz, S. (2001) Experimental Verification of a Negative Index of Refraction. *Science*, **292**, 77-79.  
<https://doi.org/10.1126/science.1058847>
- [4] Sievenpiper, D.F., Schaffner, J.H., Song, H.J., *et al.* (2003) Two-Dimensional Beam Steering Using an Electrically Tunable Impedance Surface. *IEEE Transactions on Antennas and Propagation*, **51**, 2713-2722.  
<https://doi.org/10.1109/TAP.2003.817558>

- [5] Costa, F., Monorchio, A., Talarico, S., et al. (2008) An Active High-Impedance Surface for Low-Profile Tunable and Steerable Antennas. *IEEE Antennas and Wireless Propagation Letters*, **7**, 676-680. <https://doi.org/10.1109/LAWP.2008.2006070>
- [6] Hong, J., Kim, Y. and Yoon, Y. (2013) Tunable Electromagnetic Gradient Surface for Beam Steering by Using Varactor Diodes. 2013 *Proceedings of the International Symposium on Antennas & Propagation (ISAP)*, Nanjing, October 2013, Vol. 2, 1211-1214.
- [7] Ratni, B., de Lustrac, A., Piau, G.P., et al. (2018) Active Metasurface for Reconfigurable Reflectors. *Applied Physics A*, **124**, Article No. 104. <https://doi.org/10.1007/s00339-017-1502-4>
- [8] Hassan, A., Fadlallah, N., Rammal, M., Nashef, G. and Rachid, E. (2021) Wideband Reconfigurable Millimeter-Wave Linear Array Antenna Using Liquid Crystal for 5G Networks. *Wireless Engineering and Technology*, **12**, 1-14. <https://doi.org/10.4236/wet.2021.121001>
- [9] Mavridou, M. and Feresidis, A.P. (2016) Dynamically Reconfigurable High Impedance and Frequency Selective Metasurfaces Using Piezoelectric Actuators. *IEEE Transactions on Antennas and Propagation*, **64**, 5190-5197. <https://doi.org/10.1109/TAP.2016.2617372>
- [10] Vassos, E., Churm, J. and Feresidis, A. (2020) Ultra-Low-Loss Tunable Piezoelectric-Actuated Metasurfaces Achieving 360° or 180° Dynamic Phase Shift at Millimeter-Waves. *Scientific Reports*, **10**, Article No. 15679. <https://doi.org/10.1038/s41598-020-72874-y>
- [11] Rotshild, D. and Abramovich, A. (2021) Ultra-Wideband Reconfigurable X-Band and Ku-Band Metasurface Beam-Steerable Reflector for Satellite Communications. *Electronics*, **10**, Article No. 2165. <https://doi.org/10.3390/electronics10172165>
- [12] Li, A., Singh, S. and Sievenpiper, D. (2018) Metasurfaces and Their Applications. *Nanophotonics*, **7**, 989-1011. <https://doi.org/10.1515/nanoph-2017-0120>
- [13] Litmanovitch, G., Rotshild, D. and Abramovich, A. (2017) Flat Mirror for Millimeter-Wave and Terahertz Imaging Systems Using an Inexpensive Metasurface. *Chinese Optics Letters*, **15**, Article ID: 011101. <https://doi.org/10.3788/COL201715.011101>
- [14] Chang, K., Ahn, J. and Yoon, Y.J. (2009) Physically Flat but Electromagnetic Parabolic Surface Using EBG Structure with Stepped Reflection Phase. *IEEE Antennas and Propagation*, 2609.
- [15] Wang, Z., Liao, D., Zhang, T., Chen, T., Ruan, Y. and Zheng, B. (2019) Metasurface-Based Focus-Tunable Mirror. *Optics Express*, **27**, 30332-30339. <https://doi.org/10.1364/OE.27.030332>